# TORSIONAL INSTABILITY OF CANTILEVERED BARS SUBJECTED TO NONCONSERVATIVE LOADING*

by

S. Nemat-Nasser
Post-doctoral Research Fellow
Department of Civil Engineering
The Technological Institute
Northwestern University
Evanston, Illinois

and

G. Herrmann
Professor of Civil Engineering
The Technological Institute
Northwestern University
Evanston, Illinois



*This research was supported by the National Aeronautics and Space Administration under Grant NsG 605.

ABSTRACT

15419

A cantilevered bar of uniform cross-section and subjected at the free end to distributed, nonconservative, compressive loads is considered. It is shown that for certain cross-sections stability may be lost by either torsional divergence (torsional buckling) or torsional flutter, depending upon the load distribution at the end section. In addition, transverse flutter can also occur. It is also indicated how such systems may be realized by means of pipes conveying fluid. Author

## 1. Introduction

The problem of the stability of a cantilevered elastic bar subjected to a compressive partial follower load at its free end has been treated recently in detail by several authors [1, 2]*. In these studies, it has been established that the bar may become unstable either by divergence (adjacent equilibrium exists) or by flutter (oscillations with increasing amplitude), depending upon the extent to which the load follows the end-rotation of the bar.

It is also well known that a compressed column may lose stability either by transverse deflection (Euler case) or by rotation of each cross-section, the axis remaining straight (torsional buckling), depending upon the shape of the cross-section [3].

The purpose of this study is to show that a cantilevered bar subjected to follower forces and possessing a suitable cross-section may lose stability either by torsional divergence (torsional buckling), torsional flutter, or transverse flutter.

To this end, we consider the system shown in Figure 1. A cantilevered bar is subjected at the free end to a pair of symmetrically applied, compressive, follower forces. The bar is assumed to have two axes of symmetry and the distance between the applied forces P and the centroid is designated by $\frac{h}{2}$. In the sequel, we shall show that, in addition to transverse flutter, the system can exhibit both torsional buckling and torsional flutter (torsional oscillations with an increasing

---

*Numbers in brackets refer to Bibliography at the end of this paper.

amplitude) depending upon the value of h .

This system may be realized by placing two pairs of very flexible pipes at the distance $\frac{h}{2}$ from the axis of rotation (z-axis in Figure 1), and pumping fluid at a constant velocity U through the pipes (see Figure 4).

## 2. Derivation of Equation of Motion and Boundary Conditions

We consider a thin-walled, cantilevered, elastic beam with length L, torsional rigidity $C = GJ$, and warping rigidity $C_1 = EC_w$ [4], subjected at the free end to a pair of compressive follower loads applied symmetrically about the centroid of the cross-section. This is shown in Figure 1, where the forces at the points A and B follow the deformation of the beam and stay tangent to the deformed longitudinal fibers at these points. The beam is assumed to have two axes of symmetry, and consequently, the equations of the lateral and torsional motions of the beam are uncoupled and may be studied independently. With the type of loading considered here, the lateral flutter of the beam occurs [5] when $2P = 20.05 \frac{EI_x}{L^2}$ *, where E is Young's modulus, and $I_x$ the least moment of inertia of the cross-section (we assume $I_y > I_x$) .

We shall use Hamilton's principle to derive the equation of torsional oscillations and the boundary conditions. With $\varphi(z,t)$ denoting the angle of rotation at section z and at time t , the strain energy of the torsional deformation is [3]

$$V_1 = \frac{1}{2}\int_0^L \left[C_1 (\varphi'')^2 + C (\varphi')^2\right] dz , \qquad (1)$$

where primes denote derivatives with respect to z . The kinetic energy is

$$T_1 = \frac{1}{2}\int_0^L mr^2 (\dot{\varphi})^2 \, dz , \qquad (2)$$

where dot denotes differentiation with respect to time, m is the mass per

---

*See Bolotin [6] for historical background and for further references.

unit of length, and r the polar radius of gyration of the cross-section of the beam.

The work done on the system by the applied compressive forces is composed of two parts. The first

$$W_1 = 2P \int_0^L \frac{1}{2} r^2 (\varphi')^2 \, dz \, , \tag{3}$$

is due to the longitudinal shortening, and the second, expressed in incremental form,

$$\delta W_2 = - P \frac{h^2}{2} \varphi'(L) \, \delta\varphi(L) \, , \tag{4}$$

is due to the moment induced by the projection of P on the x-y plane. $\delta\varphi(L)$ is the variation of the angle of rotation at the free end; $z = L$. With the Lagrangian $L = T_1 - V_1 + W_1$, Hamilton's principle may be stated as

$$\delta \int_{t_1}^{t_2} L \, dt - \int_{t_1}^{t_2} P \frac{h^2}{2} \varphi'(L) \, \delta\varphi(L) \, dt \tag{5}$$

which, after carrying out the variations and using integration by parts, yields

$$\left.\begin{aligned} & C_1 \frac{\partial^4 \varphi}{\partial z^4} + (2Pr^2 - C) \frac{\partial^2 \varphi}{\partial z^2} + mr^2 \frac{\partial^2 \varphi}{\partial t^2} = 0 \, , \\ & \varphi = \frac{\partial \varphi}{\partial z} = 0 \, ; \quad \text{at } z = 0 \, , \\ & \frac{\partial^2 \varphi}{\partial z^2} = 0 \, , \\ & C_1 \frac{\partial^3 \varphi}{\partial z^3} + \left[ P(2r^2 - \frac{h^2}{2}) - C \right] \frac{\partial \varphi}{\partial z} = 0 \end{aligned}\right\} ; \text{ at } z = L \, . \tag{6}$$

Let us note that, similar to the case of nonconservative transverse stability of a bar, the effect of nonconservative end forces in equations (6) is present only in the boundary conditions. Moreover, from the last equation in (6) we see that, for small values of h , the conservative components of the forces are more dominating (see also equation (5)) and the beam can only buckle (loss of stability by divergence). As h increases, the nonconservative effect of the follower forces becomes more pronounced and for some value of h , the mode of loss of stability shifts from buckling to that of torsional flutter. It is noted that, as in the case studied by Herrmann and Bungay [7], here too multiple regions of stability and instability may occur.

## 3. Stability Regions

A. Torsional Buckling: In order to study system (6), let us first introduce the following dimensionless quantities:

$$\zeta = \frac{z}{L} ,$$

$$\tau = t\sqrt{\frac{C_1}{mr^2L^4}} ,$$

$$\kappa = \frac{CL^2}{C_1} ,$$

$$\alpha = \frac{h}{r} ,$$

$$F = \frac{Pr^2L^2}{C_1} , \qquad \text{and} \qquad \bar{F} = 2F - \kappa .$$

Equations (6) now become

$$\frac{\partial^4\varphi}{\partial\zeta^4} + \bar{F}\frac{\partial^2\varphi}{\partial\zeta^2} + \frac{\partial^2\varphi}{\partial\tau^2} = 0 ,$$

$$\varphi = \frac{\partial\varphi}{\partial\zeta} = 0 ; \qquad \text{at } \zeta = 0 ,$$

$$\left.\begin{aligned} &\frac{\partial^2\varphi}{\partial\zeta^2} = 0 , \\ &\frac{\partial^3\varphi}{\partial\zeta^3} + \left[\bar{F}\left(1 - \frac{\alpha^2}{4}\right) - \frac{\kappa}{4}\alpha^2\right]\frac{\partial\varphi}{\partial\zeta} = 0 \end{aligned}\right\} ; \text{ at } \zeta = 1 . \qquad (7)$$

We now let $\varphi(\zeta,\tau) = e^{\lambda\zeta}\, e^{-i\omega\tau}$ ; $i = \sqrt{-1}$ , and obtain

$$\psi(\zeta) = A\ \mathrm{Sh}\ \lambda_1\zeta + B\ \mathrm{Ch}\ \lambda_1\zeta + C\ \mathrm{Sin}\ \lambda_2\zeta + D\ \mathrm{Cos}\ \lambda_2\zeta \tag{8}$$

where

$$\lambda_1^2 = -\frac{\bar{F}}{2} + \sqrt{\frac{\bar{F}^2}{4} + \omega^2}\ , \quad \lambda_2^2 = \frac{\bar{F}}{2} + \sqrt{\frac{\bar{F}^2}{4} + \omega^2}\ .$$

Substitution of (8) into the boundary conditions (7) yields a set of four homogeneous, linear equations in four constants A, B, C, and D. This set has nontrivial solutions if and only if the determinant of the coefficients is zero, i.e. the frequency equation is

$$\Delta \equiv (\lambda_1^4 + \lambda_2^4) + 2\,\lambda_1^2\,\lambda_2^2\,\mathrm{Ch}\,\lambda_1\,\mathrm{Cos}\,\lambda_2 - \lambda_1\,\lambda_2(\lambda_1^2 - \lambda_2^2)\,\mathrm{Sh}\,\lambda_1\,\mathrm{Sin}\,\lambda_2 +$$

$$+ \eta\,[(\lambda_1^2 - \lambda_2^2)(1 - \mathrm{Ch}\,\lambda_1\,\mathrm{Cos}\,\lambda_2) - 2\,\lambda_1\,\lambda_2\,\mathrm{Sh}\,\lambda_1\,\mathrm{Sin}\,\lambda_2] = 0 \tag{9}$$

where

$$\eta = \bar{F}\left(1 - \frac{\alpha^2}{4}\right) - \frac{\kappa}{4}\,\alpha^2\ .$$

To obtain the condition for divergent torsional motion, we let $\omega = 0$ ; or equivalently $\lambda_1 = 0$ , and obtain

$$\Delta(\bar{F},\alpha) = \bar{F} + \left[\ \bar{F}\left(1 - \frac{\alpha^2}{4}\right) - \frac{\kappa}{4}\,\alpha^2\ \right](\mathrm{Cos}\sqrt{\bar{F}} - 1) = 0\ . \tag{10}$$

To simplify the numerical calculations, we set

$$\bar{F} = \gamma\,\pi^2\ , \quad \kappa = \delta\,\pi^2\ , \tag{11}$$

and get

$$\alpha^2 = -\frac{4\,\gamma\,\mathrm{Cos}\,\pi\sqrt{\gamma}}{(\gamma + \delta)(1 - \mathrm{Cos}\,\pi\sqrt{\gamma})}\ . \tag{12}$$

For $\gamma = \frac{1}{4}\ ,\ \frac{9}{4}\ ,\ \ldots,\ \frac{(2n-1)^2}{4}$ , $\alpha$ is zero, and when $\frac{1}{4} \le \gamma \le \frac{9}{4}$ we

obtain the first branch (the only practically significant one) of the torsional buckling curve. This is shown in Figure 2 for $\delta = 1$ . The maximum value of $\alpha$ is obtained for $\gamma \approx 1.30$ , that is $\alpha \approx 1.04$ .

B. Torsional Flutter: For given $\alpha$ and $\bar{F} = \gamma \pi^2$ , equation (9) yields the frequencies of torsional oscillations. When $\bar{F}$ is small, these frequencies are all real. As we increase $\bar{F}$, the two lowest frequencies approach each other, and for a certain value of $\bar{F}$, say $\bar{F}_{cr.}$ , equation (9) yields a double real frequency. If we now increase $\bar{F}$ beyond this critical value, $\bar{F}_{cr.}$ , $\omega^2$ becomes complex and, therefore, one of the $\pm i\omega$ will have a positive real part. The beam will oscillate with an exponentially increasing amplitude. Consequently, we shall seek, for given $\alpha$, an $\bar{F}$ which yields a double real root of (9). This is illustrated in Figure 3 for $\alpha = 1.50$ . Similar results may be obtained for other values of $\alpha$. In this manner the torsional flutter curve may be constructed. The first branch (the only practically significant one) of torsional flutter is shown in Figure 2 for $\delta = 1$ . We note that the buckling and the flutter curves are tangent to each other at $\alpha \approx 0.975$ , $\gamma \approx 1.69$ ; that is for $\frac{h}{r} \approx 0.975$ and $P \approx 1.345\, \pi^2 \frac{C_1}{r^2 L^2}$ . $\alpha = 0.975$ is shown by a vertical dotted line in Figure 2.

The dashed line in Figure 2 indicates the limit of transverse flutter of the beam. It is assumed that $\frac{E I_x r^2}{C_1} = 1.5$ for the particular case shown in Figure 2. The regions of torsional and transverse flutter are separated by a vertical dotted line in this Figure.

## 4. Realization of Torsional Instability and of the Follower Forces

In order to realize, experimentally, the system discussed in the previous section, one must be able to subject the cantilevered beam to a system of forces which follow the deformation of the free end of the bar. This may be accomplished by incorporating into the system two pairs of very flexible pipes, which are securely attached to the bar at a distance $\frac{h}{2}$ from the z-axis (so that the whole system deforms as a unit), and pumping fluid at a constant velocity U through the pipes, as sketched in Figure 4.

We shall assume that the mass density of the fluid per unit length of each pair of the pipes is M , and a nozzle whose opening is n times smaller than the area of each pipe is also placed at the free end of each pipe.

Similar to the work of Benjamin [8], Hamilton's principle may very effectively be used for the derivation of the equation of motion and the boundary conditions. To this end, let $w(z,t)$ denote the average displacement at section z and at time t in the z-direction. The strain energy and the kinetic energy of the system (exclusive of the fluid) are given by equations (1) and (2) respectively. The total kinetic energy of the fluid may be obtained by adding to the kinetic energy of the fluid contained within the pipes, $T_2$ , the change in the kinetic energy of the fluid entering and leaving the pipes during a very small interval of the time $\Delta t$ ;

$$T' = T_2 + 2MU \left( \frac{1}{2} U_o^2 - \frac{1}{2} U_i^2 \right) \Delta t \ , \qquad (13)$$

where $T'$ is the total kinetic energy of the fluid, $\vec{U}_o$ the outlet velocity vector, and $\vec{U}_i$ the inlet velocity vector. But $\vec{U}_i = U \hat{i}$, where $\hat{i}$ is the unit vector in the z-direction, and $\vec{U}_o = \dot{\vec{r}} + n U \hat{\tau}$ where $\hat{\tau}$ is the unit vector tangent to the top (bottom) pipes at $z = L$, and $\vec{r}$ the position vector of the top (bottom) pipes at $z = L$. Hence, $\delta T'$ becomes

$$\delta T' = \delta T_2 + 2MU \left( \frac{1}{2} \dot{\vec{r}} + n U \hat{\tau} \right) \cdot \delta \vec{r} \tag{14}$$

The components of the absolute velocity of the fluid are $\dot{y} + U \frac{\partial y}{\partial z}$ in the y-direction, and $U \left(1 - \frac{1}{2} (y')^2\right) - \dot{w}$ in the z-direction. $T_2$ then becomes (within an additive constant)

$$T_2 = 2M \int_0^L \left( \frac{1}{2} \dot{y}^2 + U \dot{y} y' - U \dot{w} \right) dz .$$

But $y = \frac{h}{2} \varphi$, which yields

$$T_2 = 2M \int_0^L \left[ \frac{h^2}{8} \dot{\varphi}^2 + \frac{Uh^2}{4} \dot{\varphi} \varphi' - U \dot{w} \right] dz . \tag{15}$$

With $\hat{j}$ being the unit vector along the y-axis, we have (see Figure 4)

$$\hat{\tau} = \hat{j} \sin \theta + \hat{i} \cos \theta = \hat{j} (y')_{z=L} + \hat{i}$$

$$= \left[ \frac{h}{2} \varphi'(L) \right] \hat{j} + \hat{i} ,$$

$$\vec{r} = \hat{j} (y)_{z=L} - \hat{i} (w)_{z=L} = \left[ \frac{h}{2} \varphi(L) \right] \hat{j} - \left[ w(L) \right] \hat{i} .$$

Then

$$\left( \dot{\vec{r}} + n\, U\, \hat{\tau} \right) \cdot \delta\vec{r} \approx - n\, U\, \delta w(L) + \frac{h^2}{4} \left[ \dot{\varphi}(L) + n\, U\, \varphi'(L) \right] \delta\varphi(L) \ , \qquad (16)$$

where $\dot{w}(L)\ \delta w(L)$ is neglected (being a term of higher order). The Lagrangian now becomes

$$L = T_1 + T_2 - V_1 + 2M\, n\, U^2\, w(L) \qquad (17)$$

and Hamilton's principle takes on the form

$$\delta \int_{t_1}^{t_2} L\, dt - \int_{t_1}^{t_2} MU\, \frac{h^2}{2} \left[ \dot{\varphi}(L) + n\, U\, \varphi'(L) \right] \delta\varphi(L)\, dt = 0 \ , \qquad (18)$$

where

$$w(L) = \frac{1}{2} \int_0^L r^2\, (\varphi')^2\, dz \ .$$

Carrying out the variations and using integration by parts, we obtain

$$C_1 \frac{\partial^4 \varphi}{\partial z^4} + \left[ 2M\, n\, U^2\, r^2 - C \right] \frac{\partial^2 \varphi}{\partial z^2} + M\, U\, h^2\, \frac{\partial^2 \varphi}{\partial z \partial t} +$$

$$+ \left( m\, r^2 + M\, \frac{h^2}{2} \right) \frac{\partial^2 \varphi}{\partial t^2} = 0 \ ,$$

$$\varphi = \frac{\partial \varphi}{\partial z} = 0 \ ; \qquad z = 0 \ ,$$

$$\left. \begin{aligned} &\frac{\partial^2 \varphi}{\partial z^2} = 0 \ , \\ &C_1 \frac{\partial^3 \varphi}{\partial z^3} + \left[ M\, n\, U^2 \left( 2r^2 - \frac{h^2}{2} \right) - C \right] \frac{\partial \varphi}{\partial z} = 0 \end{aligned} \right\} ; \ z = L \ . \qquad (19)$$

Introducing the following dimensionless quantities (in addition to those introduced in the previous section)

$$\beta = \frac{M}{m} , \qquad F = \frac{M\, n\, U^2\, r^2\, L^2}{C_1} ,$$

we obtain

$$\frac{\partial^4 \varphi}{\partial \zeta^4} + [2F - \kappa] \frac{\partial^2 \varphi}{\partial \zeta^2} + \sqrt{\beta \frac{F}{n}}\, \alpha^2 \frac{\partial^2 \varphi}{\partial \zeta \partial \tau} + [1 + \tfrac{1}{2} \beta\, \alpha^2] \frac{\partial^2 \varphi}{\partial \tau^2} = 0 ,$$

$$\varphi = \frac{\partial \varphi}{\partial \zeta} = 0 ; \qquad \zeta = 0 ,$$

$$\left.\begin{aligned} &\frac{\partial^2 \varphi}{\partial \zeta^2} = 0 , \\ &\frac{\partial^3 \varphi}{\partial \zeta^3} + \left[F(2 - \frac{\alpha^2}{2}) - \kappa\right] \frac{\partial \varphi}{\partial \zeta} = 0 \end{aligned}\right\} ; \zeta = 1 . \qquad (20)$$

Equations (20) are analogous to equations (7), except for the presence of a dissipative term in the equation of motion which has an effect similar to that of viscous damping and is due to the Coriolis acceleration.

The regions of torsional buckling, in this case, are identical with the case treated in section 3. But the flutter curve will shift depending upon the values of $\beta$ and n . A complete analysis of this case is rather cumbersome and will be relegated to a separate study. Moreover, the results of an experimental investigation will also be reported elsewhere.

## 5. Discussion of Results and Conclusions

From the above study we see that the mode of loss of stability of a thin-walled cantilevered bar subjected to a set of follower forces is highly dependent upon the manner in which these forces are distributed over the end section of the bar. Although the resultant compressive force does not change, the behavior of the system may be drastically influenced by varying the end load distribution. This may seem to indicate that the present problem is an example of a system in which Saint-Venant's principle is violated. However, strictly speaking, this is not the case. The variation of the end load distributions, in the case of the follower forces, does in fact change the resultant end moment induced by the motion of the system. Therefore, the moment produced by the deformation of the bar should be taken into consideration if one wishes to compare the possible motions of the system.

In our study we have considered only the cases where $C_1 \neq 0$ (see equations (6)). For $C_1 = 0$, the system can never exhibit torsional flutter. It may either buckle (torsionally) or flutter transversely independently of the load distribution at the free end (of course, this distribution is assumed to be symmetrical about both axes of the symmetry of the cross-section of the rod).

Another class of systems which was deliberately excluded is that comprising compressed bars with one axis, or without any axes of symmetry. These cases lead to coupled torsional and bending motions which can become quite complicated and their thorough study is postponed to the future.

Similarly, the effect of the structural damping coupled with that of external damping which may lead to destabilization will be treated elsewhere.

## REFERENCES


[1] Z. Kordas and M. Życzkowski, "On the Loss of Stability of a Rod under a Super-Tangential Force," Archiwum Mechaniki Stosowanej, Vol. 1, No. 15, 1963, pp. 7-31.

[2] L. Contri, "Della Trave Caricata di Punta da Forze di Direzione Dipendente dalla sua Deformazione," Giornale de Genio Civile, 1964, pp. 32-39.

[3] F. Bleich, Buckling Strength of Metal Structures, McGraw-Hill Book Company, Inc., New York, N.Y., 1952.

[4] S. Timoshenko and J. Gere, Theory of Elastic Stability, McGraw-Hill Book Company, Inc., New York, N.Y., 1961.

[5] M. Beck, "Die Knicklast des einseitig eingespannten tangential gendrücken Stabes," Z. Angew. Math. Phys. Vol. 3, No. 3, 1952.

[6] V. V. Bolotin, Nonconservative Problems of Theory of Elastic Stability, Moscow, 1961, English translation published by Pergamon Press, Inc., New York, N.Y., 1963.

[7] G. Herrmann and R. W. Bungay, "On the Stability of Elastic Systems Subjected to Nonconservative Forces," Journal of Applied Mechanics, Vol. 31, 1964, pp. 435-440.

[8] T. B. Benjamin, "Dynamics of a System of Articulated Pipes Conveying Fluid," Proc. Roy. Soc. A, Vol. 261, 1961, pp. 457-486 (Part I).

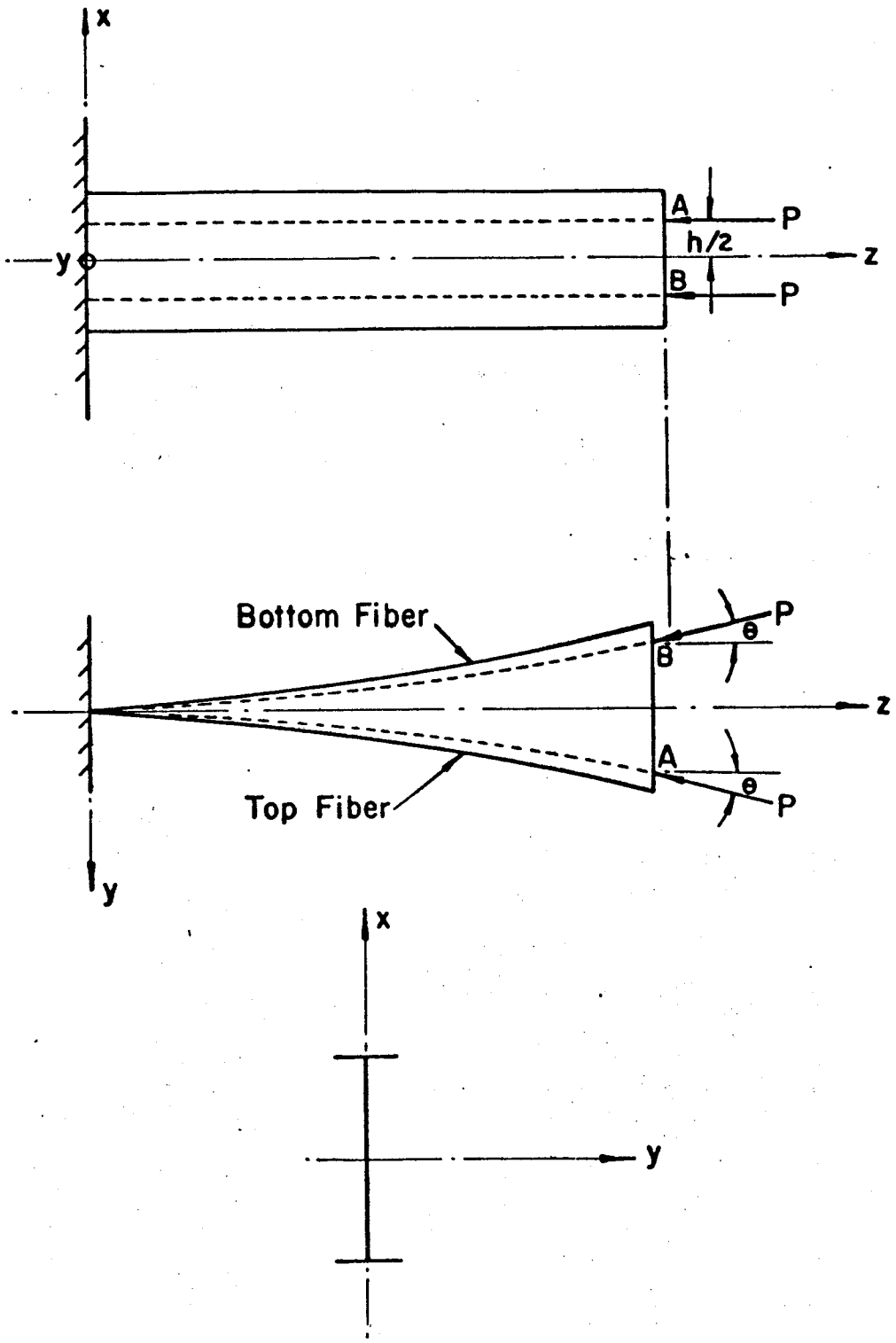


Figure 1

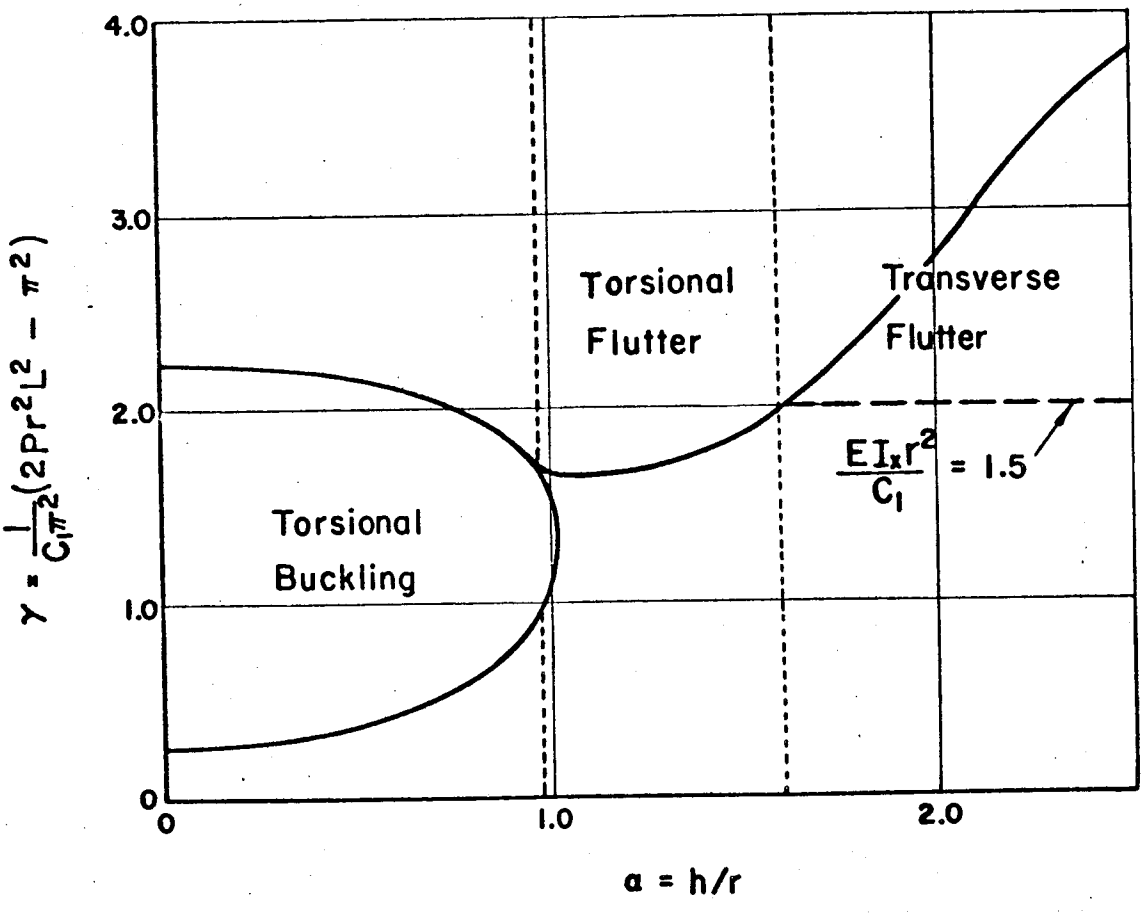


Figure 2 Stability Regions ($\delta = 1.0$)

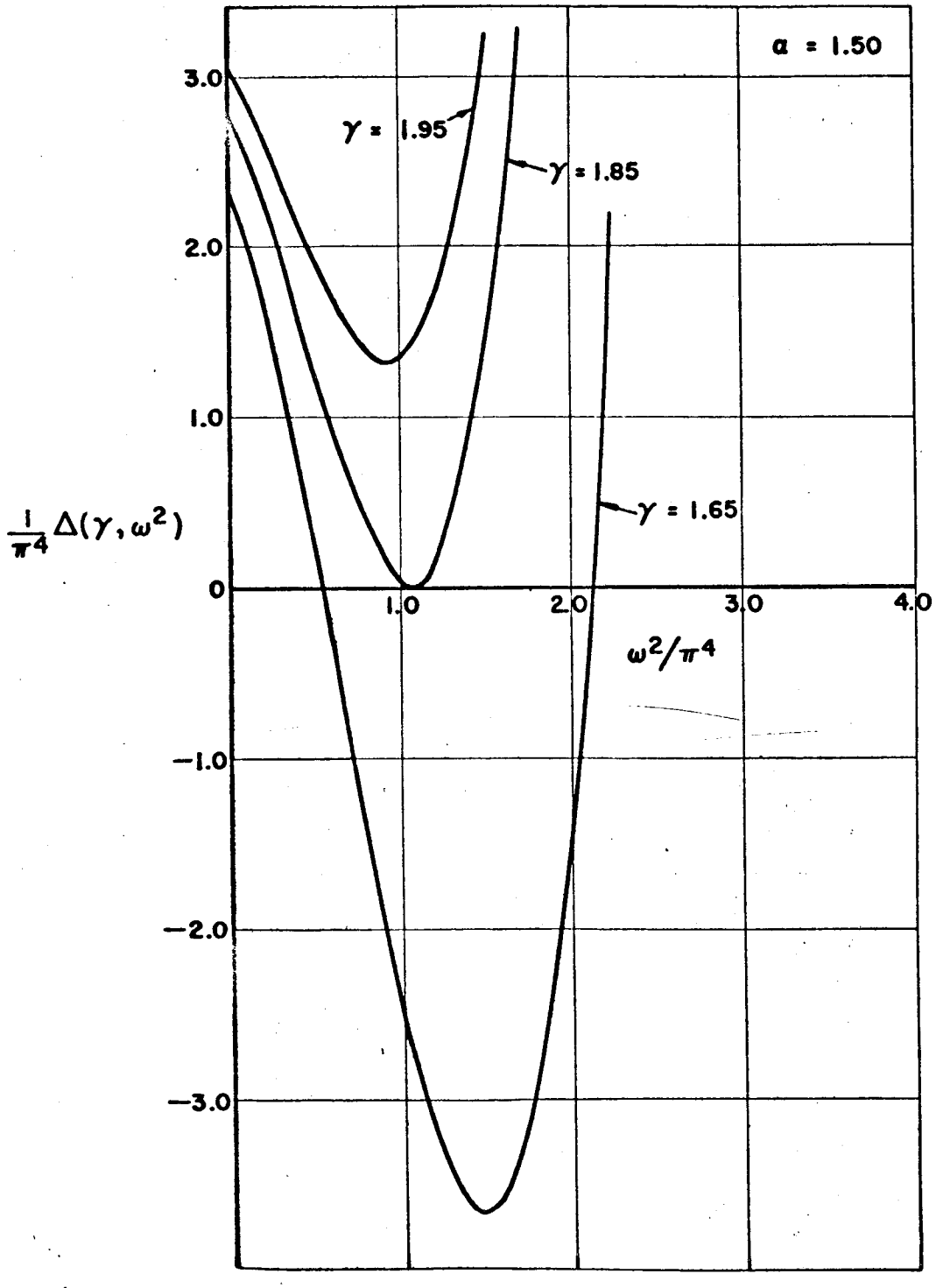
a = 1.50
γ = 1.95
γ = 1.85
γ = 1.65
3.0
2.0
1.0
0
−1.0
−2.0
−3.0
1.0
2.0
3.0
4.0
$\frac{1}{\pi^4}\Delta(\gamma,\omega^2)$
$\omega^2/\pi^4$

Figure 3

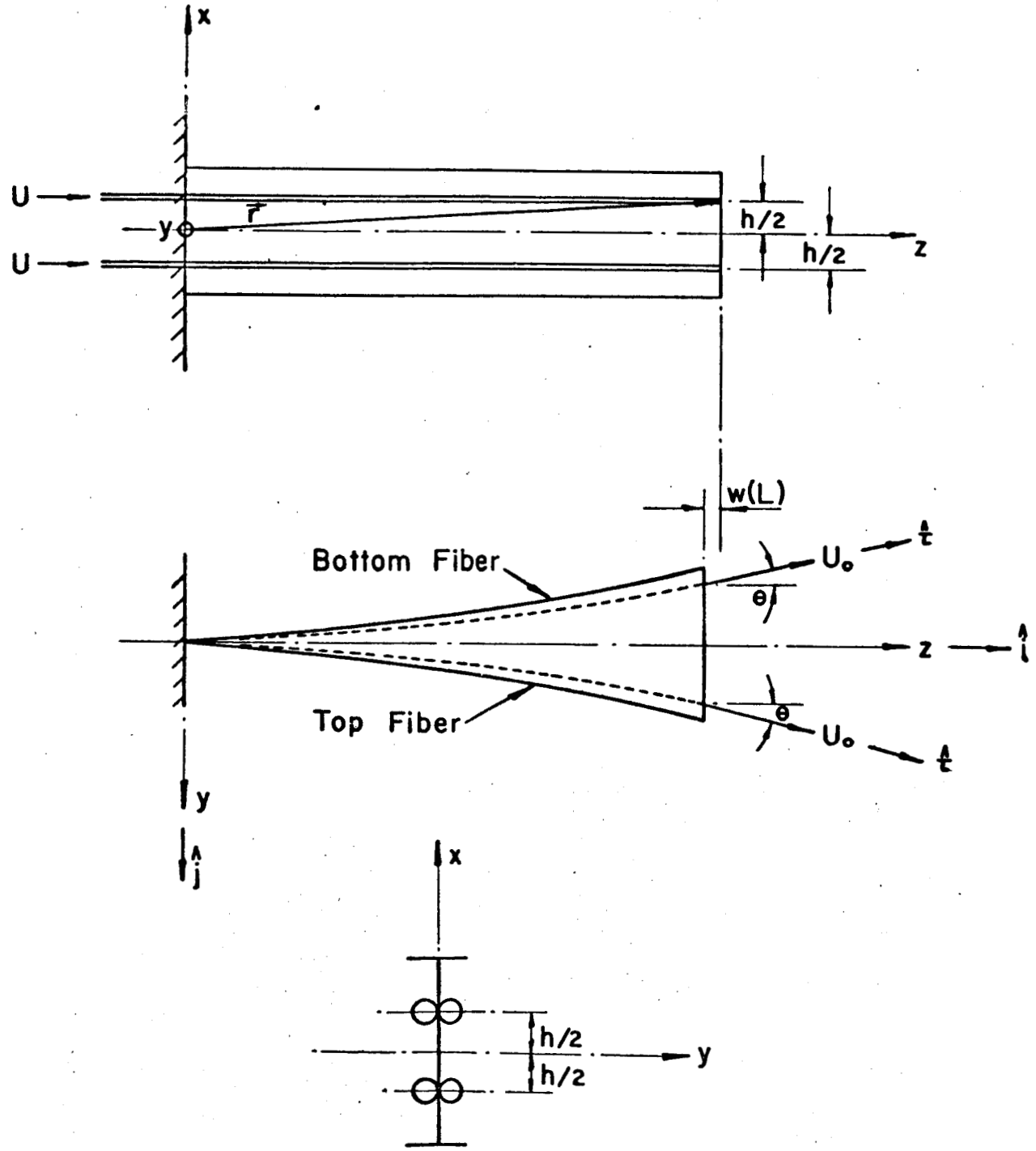


Figure 4